ELSEVIER

Journal of Quantitative Spectroscopy & Radiative Transfer 87 (2004) 1–14

Journal of Quantitative Spectroscopy & Radiative Transfer

www.elsevier.com/locate/jqsrt

Estimation of emissivities in a two-dimensional irregular geometry by inverse radiation analysis using hybrid genetic algorithm

Ki Wan Kim[a], Seung Wook Baek[a,*], Man Young Kim[b], Hong Sun Ryou[c]

[a] *Division of Aerospace Engineering, Department of Mechanical Engineering, Korea Advanced Institute of Science and Technology, 373-1, Kusong-Dong, Yusung-Gu, Taejon 305-701, South Korea*

[b] *Passenger Car Diesel Engine Test Team, Hyundai-Motor Company, Kyunggi-Do, 445-706, South Korea*

[c] *Department of Mechanical Engineering, Chung-Ang University, 221, HukSuk-Dong, DongJak-Gu, Seoul 156-756, South Korea*

Received 10 April 2003; accepted 13 August 2003

Abstract

An inverse radiation analysis is presented for estimating the wall emissivities for an absorbing, emitting, scattering media in a two-dimensional irregular geometry with diffusely emitting and reflecting opaque boundaries from the measured temperatures. The finite-volume method was employed to solve the radiative transfer equation for 2D irregular geometry. The hybrid genetic algorithm which contains local optimization algorithm was adopted to estimate wall emissivities by minimizing an objective function, while reducing computation time. It was found that an increase in the standard deviation in measurements significantly deteriorated the estimation of wall emissivities. Thus, a very accurate measurement was required in inverse radiation for better estimation of wall emissivities, especially, in a high temperature environment.

Keywords: Inverse radiation problem; Hybrid genetic algorithm; Parameter estimation; Irregular geometry; Wall emissivity

1. Introduction

Inverse radiation analysis is very practical and useful in optimizing the system, in which radiation plays an important role in manufacturing and materials processing, since the condition applied to the system can be determined from the observable results, while forward analysis only predicts the result for the input condition [1].

* Corresponding author. Tel.: +82-42-869-3714; fax: +82-42-869-3710.
E-mail address: swbaek@sorak.kaist.ac.kr (S.W. Baek).

0022-4073/$ - see front matter © 2003 Elsevier Ltd. All rights reserved.
doi:10.1016/j.jqsrt.2003.08.012

Various inverse radiation analyses have been reported for determining the extinction coefficient, the absorption coefficient, the single-scattering albedo, the phase function, or the optical thickness from radiation measurements at exit in parallel and cylindrical geometries [2–5]. Especially, the inverse source problem has been applied to parallel, spherical, cylindrical, rectangular and three-dimensional complex geometries [6–10], while the inverse analysis of the estimation of wall emissivities have been reported only in parallel plane so far [11].

Not only exit radiation measurements but also temperature measurements have been used to estimate the absorption coefficient and the scattering coefficient in three-dimensional geometry [12], while Zhou et al. [13] used exit intensity measurement for estimating temperature and radiative parameters.

In exercising inverse analysis, optimization method is usually used to minimize the errors between measured and estimated data. Among others, the least-squares method [4,11,13] and the conjugate gradient method [2,5–9,12] have been adopted. On the other hand, the genetic algorithm (GA), which is based on natural selection concept [14], is also one of the optimization methods. It has been used for parameter estimation in such applications as chemical laser modeling [15], kinetic model [16], groundwater contaminant transport model [17] and thin films [18]. Park and Froment [16] used hybrid genetic algorithm (HGA) to diminish the effects of genetic parameters such as the population size, the probability of crossover and the probability of mutation on the performance of GA. GA is different from aforementioned methods in that gradient information of objective function is not required. Li and Yang [3] applied GA to inverse radiation analysis for determining the scattering albedo, optical thickness and phase function in parallel plane.

Most of the inverse radiation analyses have been performed in cartesian coordinates. In complex geometry, the discrete ordinate method (DOM) and the finite volume method (FVM) are usually used to solve radiative transfer equation. Liu et al. [19] recommended the use of the FVM, which has advantages in selecting control angles and guaranteeing conservation of radiant energy, even though DOM and FVM are accurate and efficient in complicated high-temperature combustion systems.

In this study, the hybrid genetic algorithm is adopted for improving the efficiency of GA and reducing the effects of genetic parameters on the performance of GA. After verifying the performance of HGA, it is applied to inverse radiation analysis in estimating the wall emissivities in a two-dimensional absorbing, emitting and scattering irregular medium when the measured temperatures are given. The effects of measurement errors on the estimation accuracy are also examined.

2. Analysis

2.1. Model Description

Fig. 1 shows an irregular quadrilateral enclosure (all dimensions are in meters) which is filled with an absorbing, emitting, scattering and gray gas with $\kappa_a = 0.5\ \mathrm{m}^{-1}$ and $\sigma_s = 0.5\ \mathrm{m}^{-1}$. The nonradiative volumetric heat source is $\dot{Q} = 5.0\ \mathrm{kW/m^3}$. The walls are gray walls, and their emissivities and temperatures are all $\varepsilon_w = 0.7$ and $T = 1000\ \mathrm{K}$. The spatial and angular domains are discretized into 10×10 control volumes and 4×20 control angles which corresponds S_8 quadrature scheme [19].

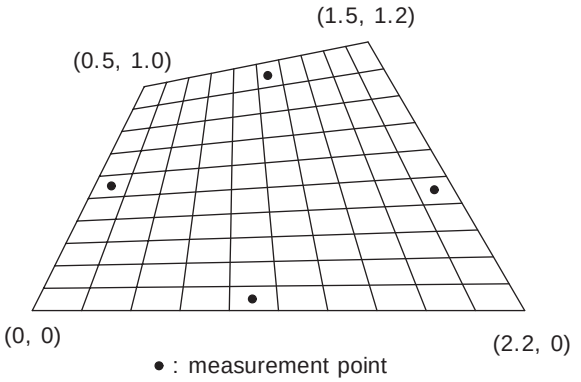

Fig. 1. Schematics of the physical system and the position of four measurement points.

The temperature distribution is determined from the energy equation [21].

$$\nabla \cdot q_r = \beta_0(1-\omega_0)\left(4\pi I_b - \sum_{n=1}^{N_\phi}\sum_{m=1}^{N_\theta} I^{mn}\Delta\Omega^{mn}\right) = \dot{Q}. \tag{1}$$

2.2. Radiative Transfer Equation (RTE)

The RTE governing radiation intensity for a gray medium at any position $\mathbf{r}$ along a path $\mathbf{s}$ through an absorbing, emitting, and scattering medium is given by

$$\frac{1}{\beta_0}\frac{\mathrm{d}I(\mathbf{r},\mathbf{s})}{\mathrm{d}s} + I(\mathbf{r},\mathbf{s}) = (1-\omega_0)I_b(\mathbf{r}) + \frac{\omega_0}{4\pi}\int_{\Omega'=4\pi} I(\mathbf{r},\mathbf{s}')\boldsymbol{\Phi}(\mathbf{s}'\to\mathbf{s})\,\mathrm{d}\Omega', \tag{2}$$

where $\beta_0 = \kappa_a + \sigma_s$ is the extinction coefficient, and $\omega_0 = \sigma_s/\beta_0$ is the scattering albedo. $\boldsymbol{\Phi}(\mathbf{s}'\to\mathbf{s})$ is the scattering phase function for radiation from incoming direction $\mathbf{s}'$ to scattered direction $\mathbf{s}$ and is approximated by a finite series of Legendre polynomial as

$$\boldsymbol{\Phi}(\mathbf{s}'\to\mathbf{s}) = \boldsymbol{\Phi}(\cos\boldsymbol{\Psi}) = \sum_{j=0}^{J} C_j P_j(\cos\boldsymbol{\Psi}), \tag{3}$$

where C_j's are the expansion coefficient, and J is the order of the phase function.

The boundary condition for a diffusely emitting and reflecting wall can be written as follows:

$$I(\mathbf{r}_w,\mathbf{s}) = \varepsilon_w I_b(\mathbf{r}_w) + \frac{1-\varepsilon_w}{\pi}\int_{\mathbf{s}'\cdot\mathbf{n}_w<0} I(\mathbf{r}_w,\mathbf{s}')|\mathbf{s}'\cdot\mathbf{n}_w|\,\mathrm{d}\Omega', \tag{4}$$

where ε_w is the wall emissivity and $\mathbf{n}_w$ is the unit normal vector to the wall.

2.3. Finite-Volume Method (FVM) for Radiation

To derive the discretization equation, Eq. (2) is integrated over a control volume, ΔV, and a control angle, $\Delta\Omega^{mn}$ as shown in Fig. 2. By assuming that the magnitude of the intensity is constant

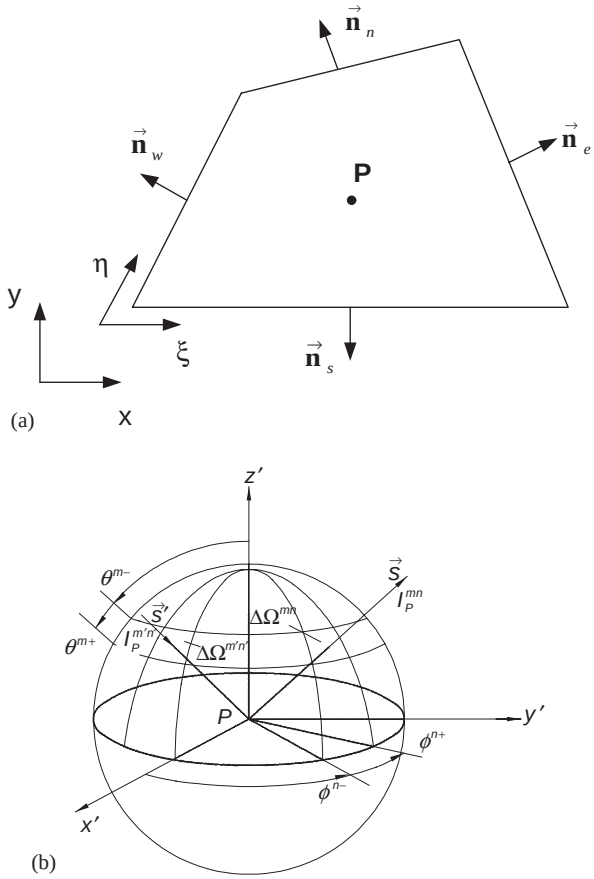

Fig. 2. Schematics of (a) control volume and (b) control angle.

but its direction varies within the control volume and control angle given, the following finite-volume formulation can be obtained

$$\sum_{i=e,w,n,s} I_i^{mn} \Delta A_i D_{ci}^{mn} = \beta_0 (-I^{mn} + S_R^{mn})_P \Delta V \Delta \Omega^m, \tag{5a}$$

where

$$D_{ci}^{mn} = \int_{\phi^{n-}}^{\phi^{n+}} \int_{\theta^{m-}}^{\theta^{m+}} (\mathbf{s} \cdot \mathbf{n}_i) \sin\theta \, \mathrm{d}\theta \, \mathrm{d}\phi, \tag{5b}$$

$$\mathbf{s} = \sin\theta \cos\phi \, \mathbf{e}_x + \sin\theta \sin\phi \, \mathbf{e}_y, \tag{5c}$$

$$\mathbf{n}_i = \mathrm{n}_{x,i} \, \mathbf{e}_x + \mathrm{n}_{y,i} \, \mathbf{e}_y, \tag{5d}$$

$$S_R^{mn} = (1-\omega_0)I_b + \frac{\omega_0}{4\pi}\int_{\Omega'=4\pi} I^{m'n'}\Phi_{m'n'\to mn}\,\mathrm{d}\Omega', \tag{5e}$$

$$\Delta\Omega^m = \int_{\phi^{n-}}^{\phi^{n+}}\int_{\theta^{m-}}^{\theta^{m+}} \sin\theta\,\mathrm{d}\theta\,\mathrm{d}\phi. \tag{5f}$$

To relate the intensities on the control-volume surfaces to a nodal one, the step scheme, which is not only simple and convenient, but also ensures positive intensity, is adopted. Then, the final discretized equation for FVM is obtained by

$$a_P^{mn} I_P^{mn} = \sum_{I=E,W,S,N} a_I^{mn} I_I^{mn} + b_P^{mn}, \tag{6a}$$

$$a_I^{mn} = -\Delta A_i D_{ci,\mathrm{in}}^{mn}, \tag{6b}$$

$$a_P^{mn} = \sum_{I=e,w,s,n} \Delta A_i D_{ci,\mathrm{out}}^{mn} + \beta_{0,P}\Delta V\Delta\Omega^{mn}, \tag{6c}$$

$$b_P^{mn} = (\beta_0 S_R^{mn})_P \Delta V\Delta\Omega^{mn}, \tag{6d}$$

where

$$D_{ci,\mathrm{out}}^{mn} = \int_{\Delta\Omega^{mn}} (\mathbf{s}\cdot\mathbf{n}_i)\,\mathrm{d}\Omega \quad \mathbf{s}\cdot\mathbf{n}_i > 0, \tag{6e}$$

$$D_{ci,\mathrm{in}}^{mn} = \int_{\Delta\Omega^{mn}} (\mathbf{s}\cdot\mathbf{n}_i)\,\mathrm{d}\Omega \quad \mathbf{s}\cdot\mathbf{n}_i < 0. \tag{6f}$$

A more detailed derivation of the transformation relations from the Cartesian coordinate to a general coordinate or other geometric relations can be easily found in the literature [20,21] so that it is recommended to refer to them for details.

2.4. Hybrid Genetic Algorithm (HGA)

Genetic algorithm (GA) is a robust parameter search technique based on the concept of natural selection. It represents and manipulates individuals at the genotype. At first generation, an initial population, which is a set of individuals that are represented in binary or float-point, is randomly generated within the range of parameters. After evaluating the fitness of each individual, fitter individuals are selected for reproducing offspring for the next generation. Selection pressure is determined by objective function values. Some of the selected individuals are chosen to find mates and undergo the crossover operation, which is a reproduction process that makes offspring by exchanging their genes to improve the fitness of the next generation. Then, some of offspring are chosen for mutation operation that keeps diversity of a population, while searching the design space that cannot be represented with present population by changing some of genes of selected individual within the range of design space. Because there is no guarantee that GA produces monotonic improvement in objective function value with variance of generation due to its stochastic nature of GA, an elitist strategy is used to ensure a monotonic improvement by copying a best individual of the present generation onto the next generation.

Unlike the calculus-based method, GA does not depend on the existence of derivatives as well as initial values. Thus, GA is very attractive for application when the objective function is highly nonlinear and multimodal like in this study. Even with these attractive features, GA has some drawbacks such as inability to perform fine local tuning and premature convergence to a non-global optimum [14]. To overcome these difficulties, improved genetic operators of selection, crossover and mutation are adopted. Additionally, a local optimization algorithm is included in GA, which is thereby called HGA.

A detailed description of the technique adopted in this study is as follows. Since the float-point representation, that renders GA closer to the problem space, is used, the string length is reduced to the number of design variables. In the float-point representation, all parameters are represented by a vector of real numbers. In this study, the population size is fixed on 10 to reduce computation time so that GA can be converged to a super-individual which is superior to the other individuals. To prevent this possibility, the stochastic universal sampling, which maintains the diversity of individuals, is adopted. For a crossover operation, the blend crossover (BLX-α) is used. BLX-0.5 is usually used, since both exploration of good solutions and exploitation of the design space are equally performed. Nonuniform mutation is also adopted here to improve local tuning. After determining the elite individual, a LOA is applied to only elite individual to reduce computation time. Efficiency is also improved by giving the chance that GA searches a better solution which LOA cannot find. Following process, which is used for non-uniform mutation having local tuning ability in [14], is adopted for LOA used in this inverse radiation study. If $\boldsymbol{s} = \langle v_1, v_2, \ldots, v_m \rangle$ is a chromosome of elite individual and the gene v_k is selected for local optimization, the resulting gene v'_k is as follows:

$$v'_k = \begin{cases} v_k + \Delta(t, UB - v_k), \\ v_k - \Delta(t, v_k - LB), \end{cases} \tag{7}$$

where LB and UB are lower and upper domain bounds of the gene v_k.

The function $\Delta(t, y)$ returns a value in the range $[0, y]$ such that the probability of $\Delta(t, y)$ being close to 0 increases as t increases. This property causes the operator to uniformly search the space initially (when t is small), and very locally at later stages. The following function is used for $\Delta(t, y)$ [14].

$$\Delta(t, y) = y \cdot (1 - r^{(1 - t/T_{\max})}), \tag{8}$$

where r is a uniform random number, $T_{\max}$ is the maximum generation number, and b is a system parameter for determining the degree of dependency on generation number, t ($b = 1$ here). In LOA, using Eq. (7) v'_k is calculated for each gene of elite individual. If v'_k is fitter than v'_k, gene of elite individual is changed to v'_k. Otherwise, v'_k is maintained. The algorithm used in this study is presented in Fig. 3.

2.5. Inverse Analysis Procedure

In this inverse radiation analysis, the emissivities are regarded as unknown while other values such as the absorption coefficient, the scattering coefficient, the temperatures at boundaries, and nonradiative volumetric heat source are assumed to be known. They can be estimated by minimization

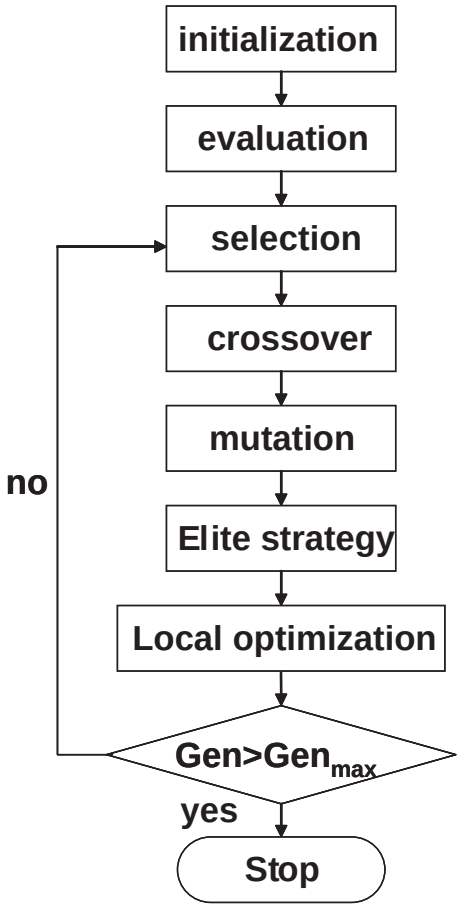

Fig. 3. The flowchart of hybrid genetic algorithm.

of objective function, which is expressed by the sum of square errors between estimated and measured temperatures at only four measurement data positions as in Fig. 1. The number of measured data points is minimized to avoid averaging error effect such that a large error of one point can average out to a reasonably small overall error when the other data is very well matched [15]. The position of data points is also selected not only to avoid averaging error effect but also to represent this system effectively with only four data points. The objective function for minimization is defined as follows:

$$f = \sum_{i=1}^{4} (T_{i,\text{measured}} - T_{i,\text{estimated}})^2. \tag{9}$$

A HGA is adopted for minimization of objective function, (9). Therefore, the emissivities are variables to be estimated in HGA.

3. Results and discussion

3.1. The performance of Local optimization algorithm (LOA)

First of all, without measurement errors, the performance of LOA is investigated. The performance of GA with/without LOA is compared with for a test that is conducted with three different initial guesses, i.e., with three different random seeds. As shown in Fig. 4, the GA with LOA minimizes the objective function, i.e., best fitness faster than the GA without LOA. In other words, the LOA improve the local tuning ability of GA. Additionally, it has a stronger dependence on random seed than the GA without LOA due to its dependence on uniform random number.

In Fig. 5, the effect of probability of crossover on HGA is examined with various probabilities of crossover of 0.25, 0.45, and 0.6. There are no significant differences among the results of various probabilities of crossover in best & average fitness. This is due to the fact that the LOA reduces the effect of probability of crossover on performance of GA.

Various probabilities of mutation of 0.1, 0.3, and 0.55 are applied to investigate the effect of probability of mutation on HGA. In Fig. 6, a lower probability of mutation seems to perform better in average fitness. However, the final best fitness converged is observed to be regardless of the mutation due to the LOA. Thus, it is again confirmed that the LOA diminishes the effect of GA parameter on its performance.

The effects of population size on best and average fitness and computation time are represented in Figs. 7 and 8, respectively. As in Fig. 7, the population size of 10 shows a best performance in a reduction of best and average fitness due to LOA. As population size decreases, the average fitness is easily affected by best individual so that the average fitness for population of 10 fluctuates more than those for any others. Population size is also proportional to

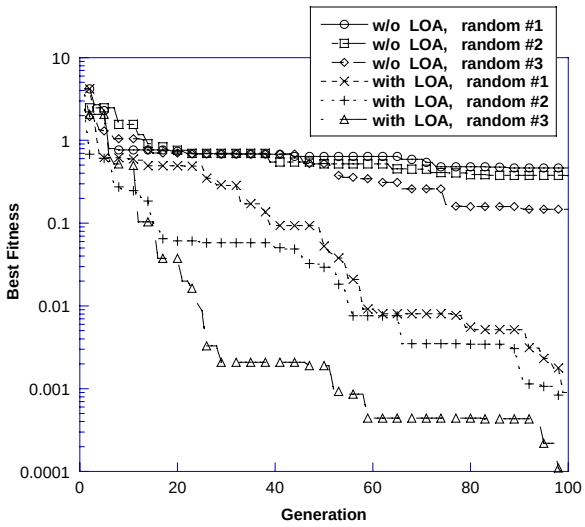

Fig. 4. Comparison of best fitness of GA without LOA and with LOA for different random seeds.

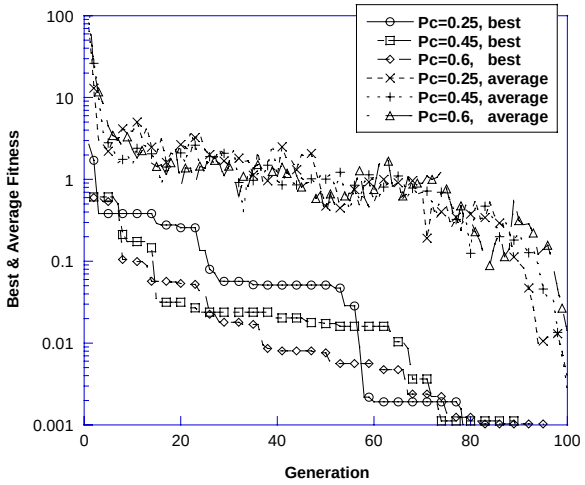

Fig. 5. Best and average fitness history for various probabilities of crossover.

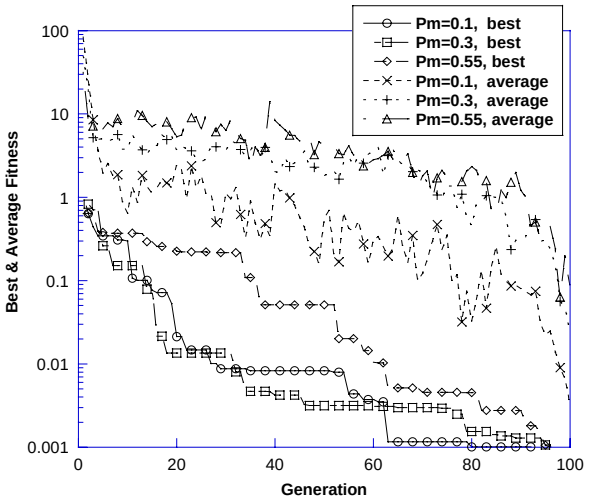

Fig. 6. Best and average fitness history for various probabilities of mutation.

computation time in GA as shown in Fig. 8. The shortest computation time again corresponds to the population size of 10. Based on these facts, a population size of 10 is chosen in forthcoming analyses.

Because the moving distance of each gene of elite chromosome in LOA is randomly determined by a ratio of generation to maximum generation, maximum generation has to be decided in advance. Since the maximum generation is also proportional to computation time in GA as shown in Fig. 9, the effect of maximum generation on the performance of GA is investigated together with computation time required in order to select a proper maximum generation. In Fig. 10, the results for maximum

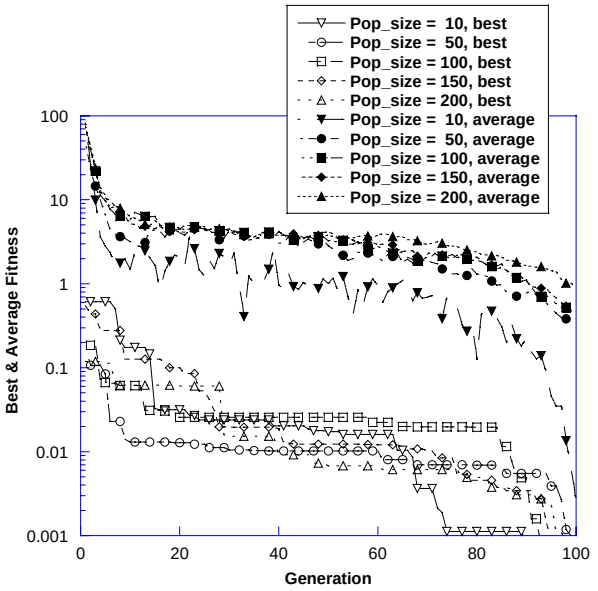

Fig. 7. Best and average fitness history for various population size.

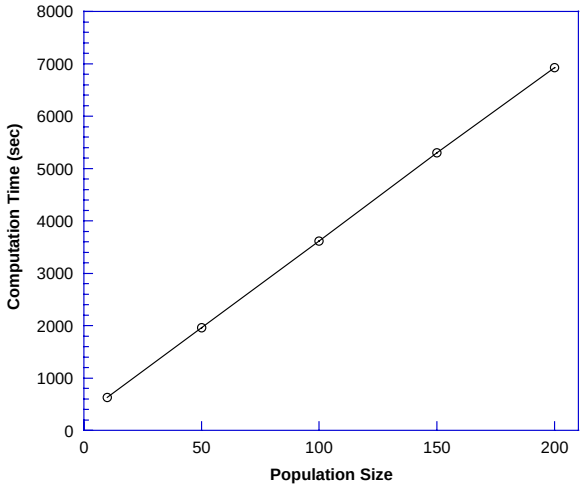

Fig. 8. Variation of computation time for different population size.

generation bigger than 100 show a good performance so that the maximum generation of 100 is selected for analysis below.

3.2. Parameter estimation of emissivities

Now, using HGA, the effect of measurement errors on accuracy of the estimation is examined. For estimating measurement error, the following relations have been usually used in inverse radiation

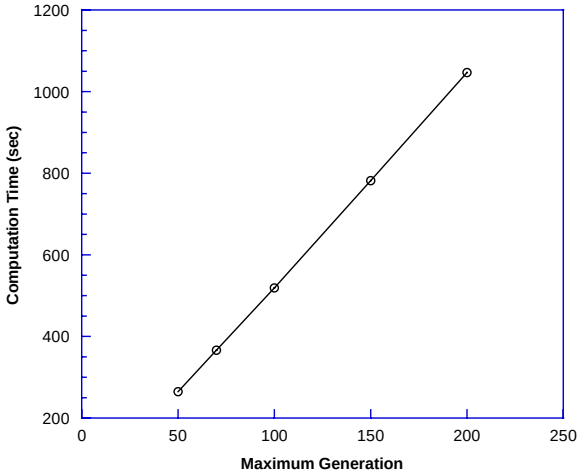

Fig. 9. Variation of computation time for different maximum generation numbers.

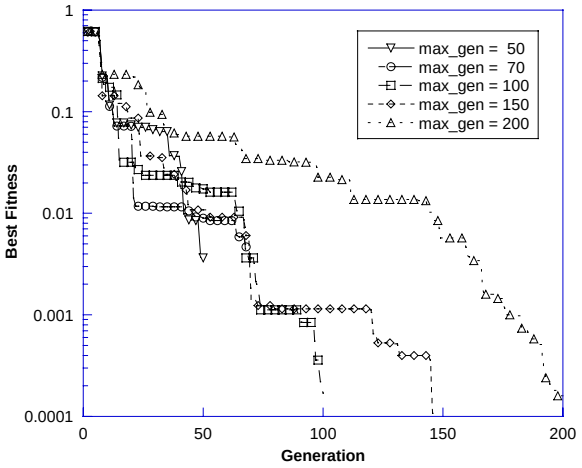

Fig. 10. Best fitness histories for various maximum generation numbers.

analysis [9].

$$(T_i)_{\text{measured}} = (T_i)_{\text{exact}} + \sigma_{\text{st}}\zeta \quad i = 1, 2, 3, 4, \tag{10}$$

where σ_{st} is a standard deviation of measurement data, and ζ is a standard normal distribution random variable. Thus, the probability that ζ is included between -2.576 and 2.576 is 99% [22]. σ_{st} can be related to relative measurement error, ε_{rel}, as follows:

$$\sigma_{\text{st}} = \frac{T_{\text{exact}} \times \varepsilon_{\text{rel}}}{2.576}. \tag{11}$$

Table 1
Estimated emissivities and averaged relative errors for different standard deviations

Parameter	True value	$\sigma = 0$		$\sigma = 0.05$		$\sigma = 0.1$	
		HGA	$\varepsilon_{rel}(\%)$	HGA	$\varepsilon_{rel}(\%)$	HGA	$\varepsilon_{rel}(\%)$
ε_1	0.7	0.7003	0.04	0.6843	2.25	0.6711	4.13
ε_2	0.7	0.7015	0.21	0.6876	1.76	0.6752	3.54
ε_3	0.7	0.6991	0.13	0.6908	1.31	0.6811	2.70
ε_4	0.7	0.7001	0.01	0.6905	1.35	0.6807	2.75
$\bar{\varepsilon}_{rel}$			0.097		1.67		3.28

Parameter	True value	$\sigma = 0.5$		$\sigma = 1$		$\sigma = 2$	
		HGA	$\varepsilon_{rel}(\%)$	HGA	$\varepsilon_{rel}(\%)$	HGA	$\varepsilon_{rel}(\%)$
ε_1	0.7	0.5718	18.31	0.4844	30.80	0.3642	47.96
ε_2	0.7	0.5905	15.65	0.5189	25.87	0.3999	42.87
ε_3	0.7	0.6177	11.76	0.5447	22.18	0.4476	36.05
ε_4	0.7	0.6076	13.20	0.5294	24.38	0.4403	37.09
$\bar{\varepsilon}_{rel}$			14.73		25.81		40.99

For error analysis, the relative and averaged relative error are defined by
Relative error

$$\varepsilon_{rel,i} = \frac{\varepsilon_{estimated,i} - \varepsilon_{exact,i}}{\varepsilon_{exact,i}} \times 100, \quad i = 1,2,3,4. \tag{12}$$

Averaged relative error

$$\bar{\varepsilon}_{rel} = \frac{\sum_{i=1}^{4} \varepsilon_{rel,i}}{4}. \tag{13}$$

After five independent computations with different initial values, the values for each parameter are averaged, since HGA is strongly dependent on random seed. Without measurement errors, the averaged relative error becomes almost negligible.

The effect of measurement error on the accuracy of the estimation is examined for various standard deviations. Table 1 shows that the accuracy of estimation of wall emissivities is sensitive to an increase in standard deviation. A typical computation time required is about 8 minutes on a personal computer with an Intel Pentium IV 2 GHz processor. According to Table 1, the standard deviation of 2 corresponds to a possible maximum measurement error of 0.5%. However, the averaged relative error for the wall emissivities is found to be about 40% for this case. In this study, the standard deviation is comparatively bigger than measurement relative error, while it is vice versa in other studies. This difference is due to the very high temperature involved in this study, i.e. about 1000 K. Thus, a more accurate temperature measurement is required to predict the wall emissivity in a high temperature environment.

4. Conclusions

An inverse radiation analysis was carried out for estimating the wall emissivities for an absorbing, emitting and scattering media in a two-dimensional irregular geometry with diffusely emitting and reflecting opaque boundaries, when the measured temperatures were given.

The finite-volume method was employed to solve the radiative transfer equation for 2D irregular geometry. A hybrid genetic algorithm, which is known for reducing the effect of genetic parameters on the performance of genetic algorithm, was adopted to estimate wall emissivities by minimizing an objective function, which is expressed by the sum of square errors between estimated and measured temperatures at only four data positions. The local optimization algorithm was applied to reduce computation time.

The effects of measurement errors on the accuracy of estimation were carefully examined. It was found that without measurement errors, the wall emissivities were accurately estimated. However, even with small measurement errors, the estimation error in predicting wall emissivities could become significant when the temperature involved was rather high. Also the result indicated that the accuracy in the estimation of wall emissivities was sensitive to increase in measurement errors. Consequently, in inverse radiation analysis a more accurate measurement in temperature was indispensable for better estimation of wall emissivities, especially, in a high temperature environment.

Acknowledgements

This research was performed for the Carbon Dioxide Reduction & Sequestration Center, one of 21st Century Frontier R& D Programs funded by the Ministry of Science and Technology of Korea.

References

[1] Jones MR. Inverse analysis of radiative heat tranfer systems. J Heat Transfer 1999;121:481–4.
[2] Li HY, Ozisik MN. Inverse radiation problem for simultaenous estimation of temperature profile and surface reflectivity. J Thermophys Heat Transfer 1993;7:88–93.
[3] Li HY, Yang CY. A genetic algorithm for inverse radiation problems. Int J Heat Mass Transfer 1997;40:1545–9.
[4] Ou NR, Wu CH. Simultaneous estimation of extinction coefficient distribution, scattering albedo and phase function of a two-dimensional medium. Int J Heat Mass Transfer 2002;45:4663–74.
[5] Li HY, Ozisik MN. Identification of the temperature profile in an absorbing, emitting, and isotropically scattering medium by inverse analysis. J Heat Transfer 1992;114:1060–3.
[6] H LL, Heping T, Qizheng Y. Inverse radiation problem in one-dimensional semitransparent plane-parallel media with opaque and specularly reflecting boundaries. JQSRT 2000;64:395–407.
[7] Li HY. A two-dimensional cylindrical inverse source problem in radiative transfer. JQSRT 2001;69:403–14.
[8] Li HY. An inverse source problem in radiative transfer for spherical media. Numer Heat Transfer, Part B 1997;31: 251–60.
[9] Liu LH, Tan HP. Inverse radiation problem in three-dimensional complicated geometric systems with opaque boundaries. JQSRT 2001;68:559–73.
[10] Li HY. Inverse radiation problem in two-dimensional rectangular media. J Thermophys Heat Transfer 1997;11: 556–61.
[11] Liu LH, Tan HP, Yu QZ. Simultaneous identification of temperature profile and wall emissivities in one-dimensional semitransparent medium by inverse radiation analysis. Numer Heat Transfer, Part A 1999;36:511–25.

[12] Park HM, Yoon TY. Solution of the inverse radiation problem using a conjugate gradient method. Int J Heat Mass Transfer 2000;43:1767–76.
[13] Zhou HC, Hou YB, Chen DL, Zheng CG. An inverse radiative transfer problem of simultaneously estimating profiles of temperature and radiative parameters from boundary intensity and temperature measurements. JQSRT 2002;74: 605–20.
[14] Michalewicz Z, Genetic algorithms + data structures = evolution programs, 3rd rev. and extended ed. New York: Springer, 1999.
[15] Carroll DL. Chemical laser modeling with genetic algorithms. AIAA J 1996;34:338–46.
[16] Park TY, Froment GF. A hybrid genetic algorithm for the estimation of parameters in detailed kinetic models. Comput Chem Eng 1998;22:S103–10.
[17] Orain S, Scudeller Y, Garcia S, Brousse T. Use of genetic algorithms for the simultaneous estimation of thin films thermal conductivity and contact resistances. Int J Heat Mass Transfer 2001;44:3973–84.
[18] Giacobbo F, Marseguerra M, Zio E. Solving the inverse problem of parameter estimation by genetic algorithms: the case of a groundwater contaminant transport model. Ann Nucl Energy 2002;29:967–81.
[19] Liu J, Shang HM, Chen YS, Wang TS. Prediction of radiative transfer in general body-fitted coordinates. Numer Heat Transfer, Part B 1997;31:423–39.
[20] Chai JC, Parthasarathy G, Lee HS, Patankar SV. Finite volume radiative heat transfer procedure for irregular geometries. J Thermophys Heat Transfer 1995;9:410–5.
[21] Baek SW, Kim MY, Kim JS. Nonorthogonal finite-volume solutions of radiative heat transfer in a three-dimensional enclosure. Numer Heat Transfer, Part B 1998;34:419–37.
[22] Hayter AJ. Probability and statistics for engineers and scientists, 2nd ed. Duxbury, USA, 2002.